ARTICLES

Kinetic Model for Chlorophyll Degradation in Green Tissue. 2. Pheophorbide Degradation to Colorless Compounds

Alejandro G. Marangoni*

Department of Food Science, University of Guelph, Guelph, Ontario, Canada N1G 2W1

In previous work by our group, a general mechanistic model was developed to describe chlorophyll degradation to pheophytin, chlorophyllide, and pheophorbide. This model was expanded in this work to include pheophorbide degradation to colorless degradation products and to account for incomplete pigment degradation. The model can now be utilized to help understand, and eventually help control, chlorophyll degradation in green tissue.

Keywords: *Chlorophyll; degradation; kinetics; model*

INTRODUCTION

In former work by our group (Heaton et al., 1996b), a general mechanistic mathematical model was derived for the description of chlorophyll degradation in food products and green plant tissues. In food products, chlorophyll degradation studies have shown that chlorophyll degrades to pheophorbide via either pheophytin or chlorophyllide (White et al., 1963; Gupte et al., 1963; Mahanta and Hazarika, 1985; Minguez-Mosquera et al., 1989; Heaton et al., 1996a). These, and many other studies, have basically demonstrated that chlorophyll degradation stops at pheophorbide (Schwartz and Lorenzo, 1990). However, recent studies by Matile's group (Matile et al., 1992; Ginsburg and Matile, 1993; Ginsburg et al., 1994) have shown that chlorophyll degradation in plants continues beyond pheophorbide to colorless compounds. Heaton et al. (1996a) also reported that chlorophyll degradation in whole cold-stored cabbage heads did not lead to pheophorbide accumulation, leaving the degradation of pheophorbide to colorless byproducts as the only explanation. These mechanisms are summarized in a recent review on chlorophyll catabolism by our group (Heaton and Marangoni, 1996).

The purpose of this research was to expand the general mathematical model developed in earlier work (Heaton et al., 1996b), which described chlorophyll degradation to chlorophyllide, pheophytin, and pheophorbide on the basis of chlorophyll degradation studies in coleslaw (Heaton et al. 1996a), pickles (White et al., 1963), and olives (Minguez-Mosquera et al., 1989) to include the pheophorbide degradation step.

THEORY

Thus far, chlorophyll degradation in food systems has been observed to follow two pathways:

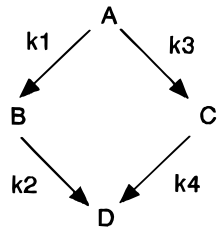

(1)

In eq 1, A is chlorophyll, B is pheophytin, C is chlorophyllide, and D is pheophorbide and the *k* terms are the rate constants for each degradation step. In recent work by our group (Heaton et al., 1996b), a kinetic model for this pathway was developed. More recently, however, chlorophyll degradation in plants has been observed to continue beyond pheophorbide [reviewed in Heaton and Marangoni (1996)]. The degradation of pheophorbide to colorless compounds should therefore also be included in the model. The new kinetic scheme for the degradation of chlorophyll in green tissue would therefore be

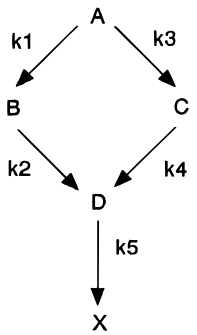

(2)

The degradation of chlorophyll outlined in eq 2 can be represented by the following set of differential

* Fax (519) 824-6631; e-mail amarango@uoguelph.ca.

S0021-8561(96)00295-6 CCC: $12.00 © 1996 American Chemical Society

equations:

$$dA/dt = -k_1A - k_3A \quad (3)$$

$$dB/dt = k_1A - k_2B \quad (4)$$

$$dC/dt = k_3A - k_4C \quad (5)$$

$$dD/dt = k_2B + k_4C - k_5D \quad (6)$$

A mass balance on all species, and the concentration of X in time, are given by

$$A_0 + B_0 + C_0 + D_0 + X_0 = A + B + C + D + X \quad (7)$$

where A_0 is the initial chlorophyll concentration, B_0 is the initial pheophytin concentration, C_0 is the initial chlorophyllide concentration, D_0 is the initial pheophorbide concentration, and X_0 is the initial, colorless, pheophorbide breakdown product concentration.

As can be appreciated in many studies on chlorophyll degradation in foods and plants, the degradation of chlorophyll, pheophytin, pheophorbide, and chlorophyllide does not always go to completion, and pigment concentration, therefore, may not decrease to zero. I have tackled this issue by introducing limits in the solution of the differential equations. Each total pigment concentration term (A_T, B_T, C_T, D_T) would therefore be composed of a fast degrading, or available (A, B, C, D), and a slow degrading, or unavailable (A', B', C', D'), pigment concentration term:

$$A_T = A + A' \qquad A_{T_0} = A_0 + A' \quad (7)$$

$$B_T = B + B' \qquad B_{T_0} = B_0 + B' \quad (8)$$

$$C_T = C + C' \qquad C_{T_0} = C_0 + C' \quad (9)$$

$$D_T = D + D' \qquad D_{T_0} = D_0 + D' \quad (10)$$

The T subscript denotes total pigment concentration at a particular time, the T_0 subscript denotes total pigment concentration at time zero, and the 0 subscript denotes available pigment concentration at time zero. Pigment concentration terms without subscripts represent fast degrading, or available, pigment concentrations at a particular time. Pigment concentration terms with a prime represent slow degrading, or unavailable, pigment concentrations (the limiting values) at a particular time. In most experiments total pigment concentrations are determined; therefore these mass balances (eqs 7−10) have to be included in the solutions of the differential equations. The question remains, however, what is the mechanistic significance of these limiting values? During senescence and tissue death, extensive membrane degradation takes place (Marangoni et al., 1996). Since chlorophyll is a membrane-associated pigment (Heaton and Marangoni, 1996), it is possible that chlorophyll or pheophytin, both lipophilic, could become entrapped in lipophilic matrices derived from the breakdown of biological membranes, such as lipid droplets, and therefore become inaccessible, or less accessible, to chlorophyllase attack. These effects could be depicted as

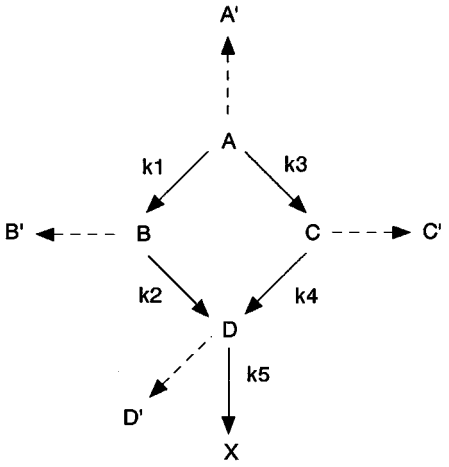

(11)

Thus, there would be slow and fast pigment degradation steps:

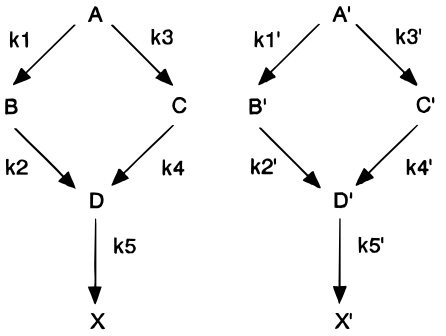

(12)

The degradation of chlorophyll, for example, could follow both pathways:

$$A = A_0\, e^{(-k_1-k_3)t} + A'_0\, e^{(-k_1'-k_3')t} \quad (13)$$

Similar equations and combinations thereof (of slow and fast steps) could be derived for pheophytin, chlorophyllide, and pheophorbide as well. Another cause for incomplete pigment degradation could be chlorophyllase inactivation. Changes in cellular environmental conditions (e.g., pH drop), proteolysis, decreased protein synthesis, and release of inhibitors due to senescent processes would cause a decrease in the amount of green pigment degrading enzyme concentrations. This would translate to time-dependent rate constants, particularly k_2, k_3, and k_5, all enzyme-mediated steps.

For example, one could include a first-order decay of these rate constants in the kinetic model

$$k = k_0\, e^{(-kt)} \quad (14)$$

The expressions derived, however, become extremely complex, and the practicality of the model is therefore lost somewhat.

The inclusion of limiting values in the differential equations is a practical strategy to deal with the incomplete degradation (in some cases) of chlorophyll, pheophytin, chlorophyllide, and pheophorbide. In the future, when the fate of chlorophyllase and the subcellular localization of chlorophyll and its degradation products are better established, modifications to the kinetic model could be pursued.

The differential equations (eqs 3−6) were simultaneously solved by integration, rearrangement, and

substitution to obtain the following set of solutions:

$$A_T = (A_{T_0} - A')\, e^{(-k_1-k_3)t} + A' \quad (15)$$

$$B_T = \frac{k_1(A_{T_0} - A')}{k_2 - k_1 - k_3}[e^{(-k_1-k_3)t} - e^{-k_2 t}] + (B_{T_0} - B')\, e^{-k_2 t} + B' \quad (16)$$

$$C_T = \frac{k_3(A_{T_0} - A')}{k_4 - k_1 - k_3}[e^{(-k_1-k_3)t} - e^{-k_4 t}] + (C_{T_0} - C')\, e^{-k_4 t} + C' \quad (17)$$

$$D_T = (D_{T_0} - D')\, e^{-k_5 t} + \frac{k_2(B_{T_0} - B')}{k_5 - k_2}[e^{-k_2 t} - e^{-k_5 t}] + \frac{k_1 k_2(A_{T_0} - A')}{(k_2 - k_1 - k_3)(k_5 - k_1 - k_3)}[e^{(-k_1-k_3)t} - e^{-k_5 t}] + \frac{k_1 k_2(A_{T_0} - A')}{(k_5 - k_2)(k_2 - k_1 - k_3)}[e^{-k_5 t} - e^{-k_2}] \times \frac{k_4(C_{T_0} - C')}{(k_5 - k_4)}[e^{-k_4 t} - e^{-k_5 t}] + \frac{k_3 k_4(A_{T_0} - A')}{(k_4 - k_1 - k_3)(k_5 - k_1 - k_3)}[e^{(-k_1-k_3)t} - e^{-k_5 t}] + \frac{k_3 k_4(A_{T_0} - A')}{(k_4 - k_1 - k_3)(k_5 - k_4)}[e^{-k_5 t} - e^{-k_4 t}] + D' \quad (18)$$

From the solutions above and the mass balance, the concentration of X can be modeled:

$$X = D_0 + A_0 + B_0 + C_0 + X_0 - A - B - C - D \quad (19)$$

MATERIALS AND METHODS

Data for modeling were obtained from White et al. (1963) for chlorophyll degradation in pickles, from Minguez-Mosquera et al. (1989) for chlorophyll degradation in olives, and from Heaton et al. (1996a) for chlorophyll degradation in white cabbage and transformed to mole percent as described in Heaton et al. (1996b). Data were fitted to the models by nonlinear least-squares methods using the software package Grafit, (Leatherbarrow, 1992). Grafit performs nonlinear regression using the method of Marquart using a numerical second-order method to calculate partial differentials (Bevington, 1969). The weighting used for determining the calculated curves was simple. Criteria for convergence was <0.01% change in the χ^2 for the fits and lack of sensitivity to different values for initial conditions (sensitivity analysis).

Values of A_{T_0}, B_{T_0}, C_{T_0}, and D_{T_0} as well as A', B', C', and D' were obtained from the data sets and fixed as constants and not included in the error minimization procedures. Whenever a pathway was not operational, the rate constant for that particular step was set to zero and fixed as a constant (eqs 11−13). Fitting pheophorbide data to our model required that all terms within eq 18 that contained rate constants or pigment concentration terms (or combinations thereof) equal to zero and that caused a particular term to become zero or undefined be removed. This procedure increased the accuracy and precision of the curve fitting procedure. It proved very difficult for eq 14 to be fitted to experimental data in its full form if some rate constants and pigment concentration terms were equal to zero.

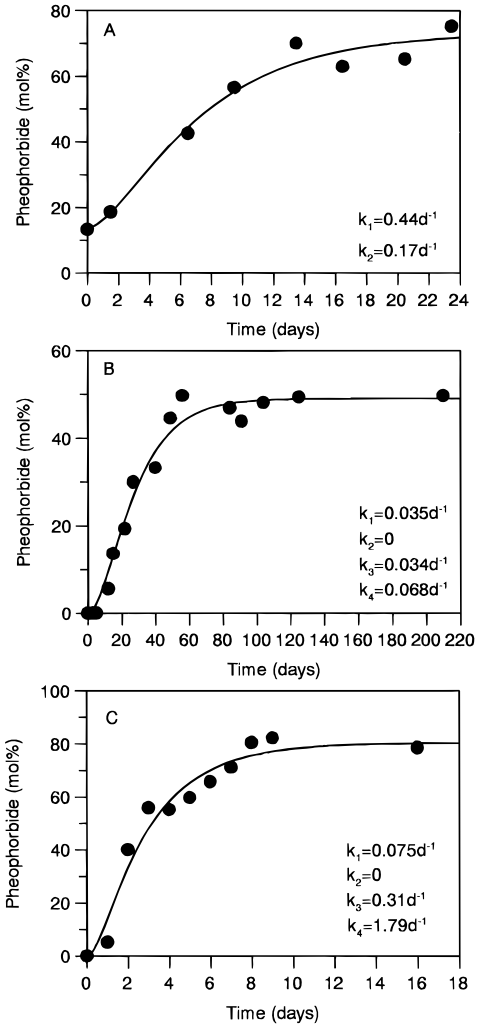

Figure 1. Accumulation of pheophorbide (mol %) in coleslaw (A), whole brined olives (B), and whole brined cucumbers as a function of time (●) and corresponding fits to the model (—) (eq 18) developed in this study.

Simulations using numerical integration for the whole degradative pathway from cholorophyll to X were performed using a fourth-order error-controlled (10^{-6} relative error, 0.01 step size) Runge−Kutta routine. The software used for this purpose was Scientist 2.0 (1995).

RESULTS AND DISCUSSION

In previous work by our group (Heaton et al., 1996b), kinetic constants for the degradation of chlorophyll to pheophytin, chlorophyllide, and pheophorbide (eq 1) in coleslaw, pickles, and green olives were derived. Limiting values were included in the calculations at that time to improve the curve fit, without any mechanistic justification. Fitting the expanded model to the experimental data resulted in rate constants almost identical to the ones reported in our previous work (Heaton et al., 1996b). This is not surprising since eqs 15−17 are identical to the ones used in that study (Heaton et al., 1996b). Rate constants derived from fitting pheophorbide data to our expanded model (eq 18) were extremely similar to those derived by Heaton et al. (1996b). The experimental data on chlorophyll degradation in coleslaw (Heaton et al., 1996a) were fitted using the following boundary conditions: $k_3 = 0$, $k_4 = 0$, $A' = 6$ mol %, $B' = 20.5$ mol %, $C' = 0.1$ mol %, $A_{T_0} = 58.4$ mol %, $B_{T_0} = 27.9$ mol %, $C_{T_0} = 0.1$ mol %, $D_{T_0} = 13.6$ mol %. Data by White et al. (1961) on brined cucumbers

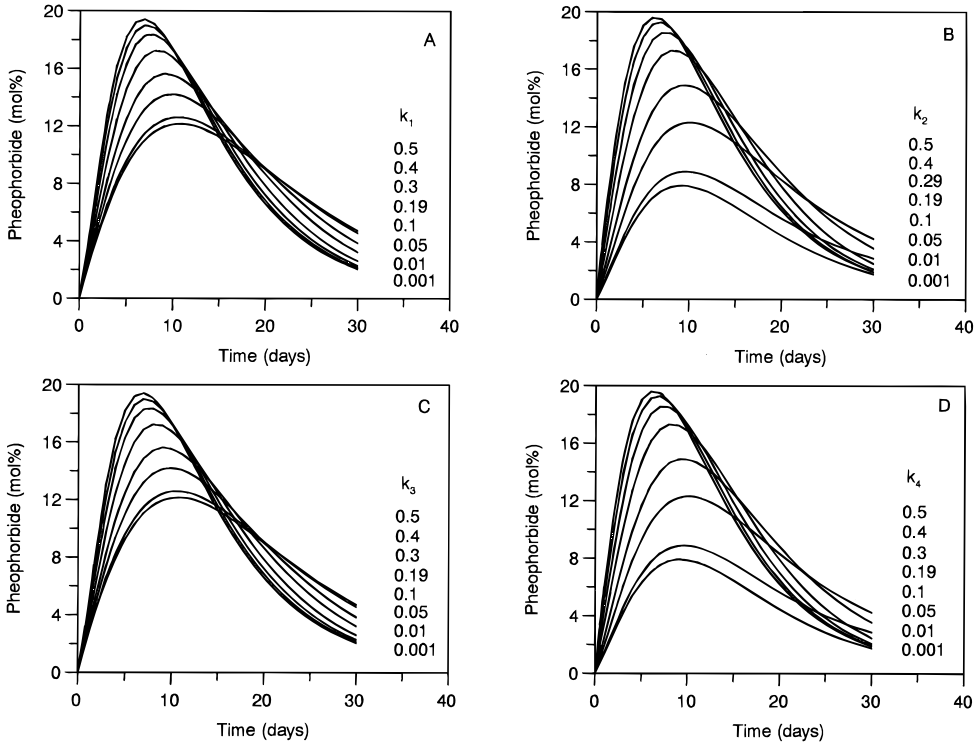

Figure 2. Simulations of the dynamics of pheophorbide accumulation (eq 18) and degradation as a function of different chosen values of the rate constants used in this model.

Table 1. Parameter and Constant Reference Values Used in the Simulations of Pheophorbide Dynamics

parameter/constant	reference value	parameter/constant	reference value	parameter/constant	reference value
k_1	0.10 day^{-1}	A_0	80 mol %	A'	5 mol %
k_2	0.12 day^{-1}	B_0	10 mol %	B'	0 mol %
k_3	0.10 day^{-1}	C_0	10 mol %	C'	0 mol %
k_4	0.12 day^{-1}	D_0	0 mol %	D'	0 mol %
k_5	0.30 day^{-1}				

were also fitted to the expanded model using the following boundary conditions: $k_2 = 0$, $A_{T_0} = 100$ mol %, $B_{T_0} = 0$, $C_{T_0} = 0$, $D_{T_0} = 0$, $A' = 0$, $B' = 21.4$ mol %, $C' = 0$, $D' = 78.6$ mol %. I also modeled Minguez-Mosquera et al.'s (1989) data on chlorophyll degradation in brined olives using the following boundary conditions: $k_2 = 0$, $A_{T_0} = 100$ mol %, $B_{T_0} = 0$, $C_{T_0} = 0$, $D_{T_0} = 0$, $A' = 0$, $B' = 50$ mol %, $C' = 0$, $D' = 50$ mol %. The calculated curves and rate constants derived from this model and the experimental data points are presented in Figure 1, demonstrating that the model described the experimental results quite accurately.

Simulations were run on pheophorbide dynamics using different values for the rate constants and limiting values (Figures 2−4). Using the reference values presented in Table 1, simulations showed how, in general, the higher the k_1-k_4, the higher the transient maximum level of pheophorbide reached. Also, the higher the transient level of pheophorbide reached, the faster the pheophorbide concentration would decrease to its limiting value (Figure 2). Increasing the value of k_5, the step that controls the conversion of pheophorbide to colorless compounds, resulted in a decreased transient accumulation of pheophorbide (Figure 3). The absence of a transient pheophorbide accumulation in the degradation of whole cabbage chlorophyll reported by Heaton et al. (1996a) may have been due to high inherent k_5 values in metabolically active tissue. Ginsburg et al. (1994) have suggested that a dioxygenase catalyzes the conversion of pheophorbide to colorless fluorescent compounds, which then are converted to

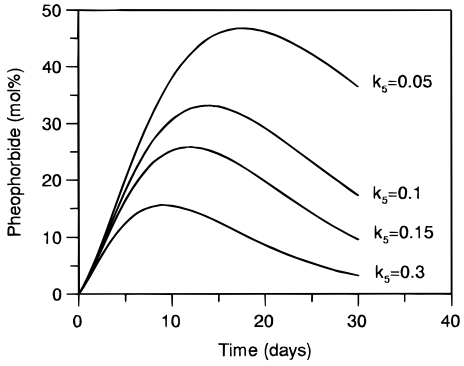

Figure 3. Simulations of the dynamics of pheophorbide accumulation (eq 18) and degradation as a function of different chosen values of the rate constant for the conversion of pheophorbide to colorless compounds (k_5).

colorless nonfluorescent compounds (Matile et al., 1992; Ginsburg and Matile, 1993; Ginsburg et al., 1994; Heaton and Marangoni, 1996). In healthy, unstressed, metabolically active tissue, therefore, it would seem that transient pheophorbide accumulations would not readily occur. Whether this is the case in food products and senescent or stressed fruits and vegetables remains to be proven. Pheophorbide dynamics for different limiting values of intermediates are shown in Figure 4.

Caution must be exercised when interpreting a dynamic pattern such as the one for pheophorbide presented in Figure 5. The figure and inset represent the same pattern, albeit at different time scales. The pattern in the inset could be interpreted as a net

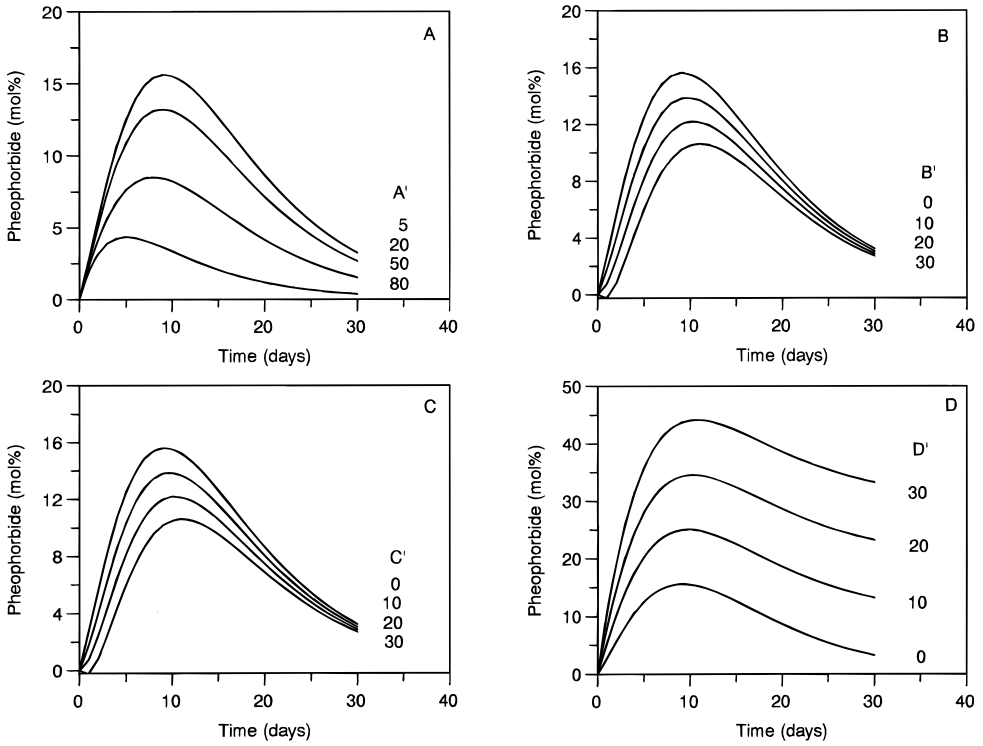

Figure 4. Simulations of the dynamics of pheophorbide accumulation (eq 18) and degradation as a function of different chosen values of the limiting intermediate concentrations used in this model.

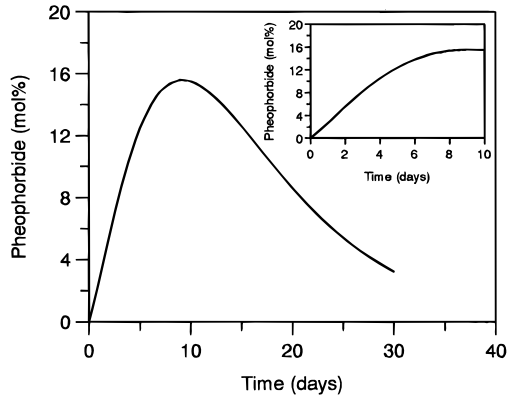

Figure 5. Simulation of the dynamics of pheophorbide accumulation and degradation (eq 18). The inset shows the same pattern viewed on a different time scale.

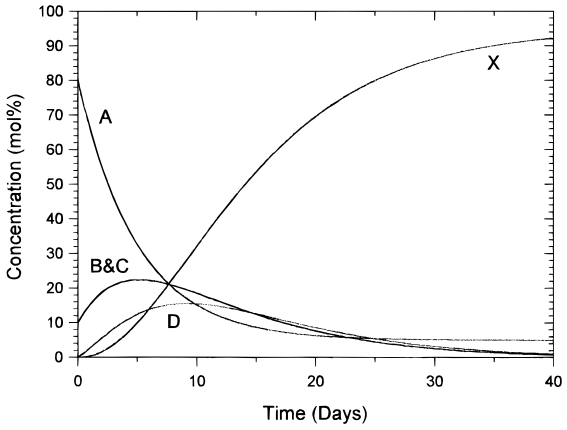

Figure 6. Simulation of whole pathway of chlorophyll degradation to colorless compounds using numerical integration: A, chlorophyll; B, pheophytin; C, chlorophyllide; D, pheophorbide; X, colorless degradation compound. Values for the rate constants used in this simulation are listed in Table 1.

accumulation of pheophorbide in time, with no evidence of breakdown to colorless compounds. However, in reality, the situation is different when longer time scales are considered.

A simulation of the whole degradative pathway at the same time using the parameters listed in Table 1 was performed and is presented in Figure 6. The patterns obtained resemble the patterns observed for chlorophyll degradation in different commodities (White et al., 1963; Minguez-Mosquera et al., 1989; Heaton et al., 1996a). As well, the numerical simulation patterns correspond closely to the patterns obtained from the simulations obtained by using the equations derived from the analytical solutions to the differential equations (Figures 2−4).

In conclusion, we have developed a complete kinetic scheme for chlorophyll degradation that includes the degradation of chlorophyll to pheophytin, chlorophyllide, pheophorbide, and ultimately colorless chlorophyll breakdown products. Future work in the area of chlorophyll degradation in food products and stressed or senescent plant tissues should include studies on the complete dynamics of chlorophyll degradation to colorless compounds and the factors regulating each step in the pathway.

LITERATURE CITED

Bevington, P. R. *Data Reduction and Error Analysis for the Physical Sciences*; McGraw-Hill: New York, 1969.

Ginsburg, S.; Matile, P. Identification of catabolites of chlorophyll-porphyrin in senescent rape cotyledons. *Plant Physiol.* **1993**, *105*, 521−527.

Ginsburg, S.; Schellenberg, M.; Matile, P. Cleavage of chlorophyll-porphyrin. *Plant Physiol.* **1994**, *105*, 545−554.

Gupte, S. M.; El-Bisi, H. M.; Francis, F. J. Kinetics of thermal degradation of chlorophyll in spinach puree. *J. Food Sci.* **1963**, *29*, 379−382.

Heaton, J. W.; Marangoni, A. G. Chlorophyll degradation in processed foods and senescent plant tissues. *Trends Food Sci. Technol.* **1996**, *7*, 8−15.

Heaton, J. W.; Yada, R. Y.; Marangoni, A. G. Discolouration of coleslaw caused by chlorophyll degradation. *J. Agric. Food Chem*. **1996a**, *44*, 395−398.

Heaton, J. W.; Lencki, R. W.; Marangoni, A. G. Kinetic model for chlorophyll degradation in green tissue. *J. Agric. Food Chem*. **1996b**, *44*, 399−402.

Leatherbarrow, R. J. Grafit version 3.0. 1992. Erithacus Software Ltd., Staines, U.K.

Mahanta, P. K.; Mazarika, M. Chlorophyll and degradation products in orthodox and CTC black teas and their influence on shade of colour and sensory quality in relation to thearubigins. *J. Sci. Food Agric.* **1985**, *36*, 1122−1139.

Marangoni, A. G.; Palma, T.; Stanley, D. W. Membrane effects in postharvest physiology. *Postharvest Biol. Technol.* **1996**, *7*, 193−217.

Matile, P.; Schellenberg, M.; Peisker, C. Production and release of chlorophyll catabolite in isolated senescent chloroplasts. *Planta* **1992**, *187*, 230−235.

Minguez-Mosquera, M. I.; Garrido-Fernández, J.; Gandul-Rojas, B. Pigment changes in olives during fermentation and brine storage. *J. Agric. Food Chem*. **1989**, *37*, 8−11.

Schwartz, S. J.; Lorenzo, T. V. Chlorophylls in foods. In *Critical Reviews in Food Science and Nutrition*; Clydesdale, F. M., Ed.; CRC: Boca Raton, FL, 1990.

Scientist 2.0. Micromath Scientific Software, Salt Lake City, UT, 1995.

White, R. C.; Jones, I. D.; Gibbs, E. Determination of chlorophylls, chlorophyllides, pheophytins and pheophorbides in plant material. *J. Food Sci.* **1963**, *28*, 431−435.

Received for review April 22, 1996. Revised manuscript received September 19, 1996. Accepted September 19, 1996.[⊗]

JF960295T

[⊗] Abstract published in *Advance ACS Abstracts,* November 1, 1996.